

Fabrication of Ordered Mesoporous Thin Films for Optical Waveguiding and Interferometric Chemical Sensing

Zhi-mei Qi,[†] Itaru Honma,[‡] and Haoshen Zhou^{*,†,‡}

PRESTO, Japan Science and Technology Agency, Kawaguchi, 332-0012, Japan, and Energy Technology Institute, National Institute of Advanced Industrial Science and Technology, Tsukuba 305-8565, Japan

Received: March 26, 2006; In Final Form: May 2, 2006

Planar optical waveguides with a propagation loss of 2.9 dB/cm at 633 nm were fabricated using ordered mesoporous thin films of $\text{TiO}_2\text{--P}_2\text{O}_5$ nanocomposite deposited on the tin-rich surfaces of float glass slides. The resulting waveguides show substantial sensitivity to parts-per-million-level ammonia gas at room temperature on the basis of single-beam polarimetric interferometry.

Waveguide-based optical chemical and biological sensors usually consist of dense and crack-free thin films that enable evanescent waves to interact with analytes over a long path length while limiting the interaction depth to the thickness of a monomolecular adlayer. Owing to this limitation, extension of the interaction path length is often needed to offer waveguide-based absorption and interferometric sensors high sensitivity.^{1,2} Sol–gel surfactant-templated mesoporous materials have a large internal surface area that is available for adsorption of molecules.^{3,4} In the case of covering the waveguiding layer with an optically transparent, ordered mesoporous thin film, the evanescent field inevitably penetrates into the film to interact with the molecules adsorbed to the pore wall. In this case, the waveguide-based sensors have an interaction depth as large as the thickness of the mesoporous film, and the sensor sensitivity per unit path length can be greatly enhanced. The sensitivity enhancement induced via an increase in the interaction depth enables the interaction path length to be reduced and consequently allows for miniaturizing the waveguide-based sensor devices. In addition to these, ordered mesoporous thin films are effective for improving other evanescent-sensing techniques such as surface plasmon resonance (SPR),⁵ optical waveguide light mode spectroscopy (OWLS),⁶ and attenuated total reflection (ATR).⁷ Moreover, by controlling pore sizes with suitable structure-directing agents, the ordered mesoporous thin films could offer waveguide-based sensors a size selectivity to chemical and biological molecules.⁸ From these points of view, one can see that ordered mesoporous thin films are advantageous to evanescent wave sensors, especially to those with a waveguide configuration. Nevertheless, up to now, ordered mesoporous thin-film optical waveguides and their applications in the field of chemical and biological sensors remain rare.⁷ In this letter, ordered mesoporous thin films of $\text{TiO}_2\text{--P}_2\text{O}_5$ (TPO) nanocomposite were fabricated onto float glass substrates via evaporation-induced self-assembly⁹ using a triblock copolymer $(\text{EO})_{20}(\text{PO})_{70}\text{-(EO)}_{20}$ (Pluronic P123) as the template. The thin films were

characterized by transmission electron microscopy (TEM), atomic force microscopy (AFM), and spectroscopic ellipsometry. The thin films deposited on the tin-rich surfaces of float glass slides were demonstrated to be planar optical waveguides with a propagation loss acceptable for use as chemical sensors. An example of the sensor application was given by using single-beam polarimetric interferometry to investigate the sensitivity of such waveguides to parts-per-million-level ammonia in dry air at room temperature.

Uniform, transparent, and ordered mesoporous thin films of TPO nanocomposite were prepared by dip-coating the cleaned glass substrates in the ethanolic solution containing TiCl_4 , $\text{PO}(\text{C}_2\text{H}_5\text{O})_3$, and P123, drying the substrates at room temperature, and finally calcining the substrates in air at 350 °C for 5 h to remove the P123 template from the films. Figure 1A shows typical small-angle X-ray diffraction (XRD) patterns of the dried and calcined films. Pattern **a** for the dried film exhibits a single peak at $2\theta = 1.08^\circ$, corresponding to $d = 8.17$ nm. This reveals that an ordered mesostructure was formed in the TPO–P123 hybrid film by evaporation-induced self-assembly during dip-coating.⁹ A single peak was also observed at $2\theta = 1.78^\circ$ in pattern **b** for the calcined film, indicating that the ordered mesostructure was maintained in the film after removal of P123 template. Calcination-induced condensation of the thin film leads to a decrease of the spacing from $d = 8.17$ nm to $d = 4.96$ nm. Refractive index and extinction coefficient of the ordered mesoporous TPO nanocomposite film in air were obtained by spectroscopic ellipsometry (Figure 1B). The film index of refraction is $n = 1.68$ at $\lambda = 633$ nm, higher than that of the glass substrate. The extinction coefficient dispersion curve indicates that the thin film is highly transparent to visible light. The findings suggest that ordered mesoporous TPO nanocomposite films coated on glass substrates can, in principle, serve as optical waveguides. The best-fitting calculations indicate that the ordered mesoporous TPO nanocomposite films are typically 226 nm thick.

TEM investigations into the film scraps peeled off the substrate also demonstrated that the ordered mesoporous mesostructure is preserved in the calcined TPO nanocomposite

* To whom correspondence should be addressed: hs.zhou@aist.go.jp.

[†] PRESTO.

[‡] Energy Technology Institute.

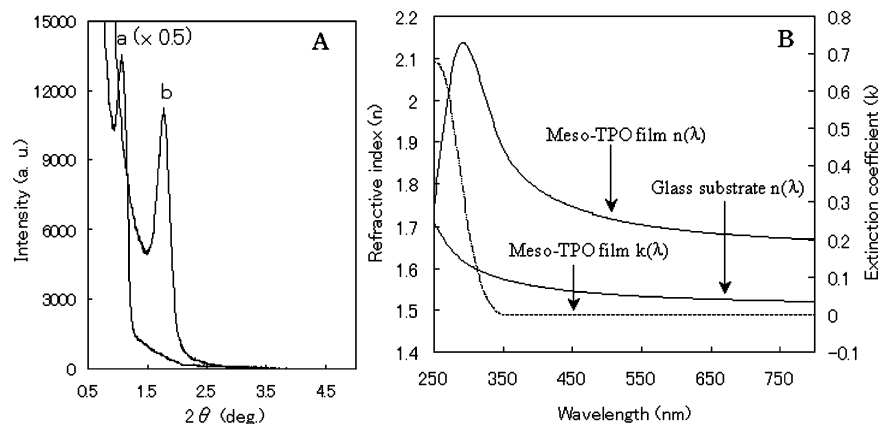


Figure 1. (A) Small-angle XRD patterns of sol-gel P123-templated TPO nanocomposite thin films before and after calcination at 350 °C (a, before; b, after). (B) Refractive index and extinction coefficient dispersion curves for the calcined film. The substrate index was also shown for comparison.

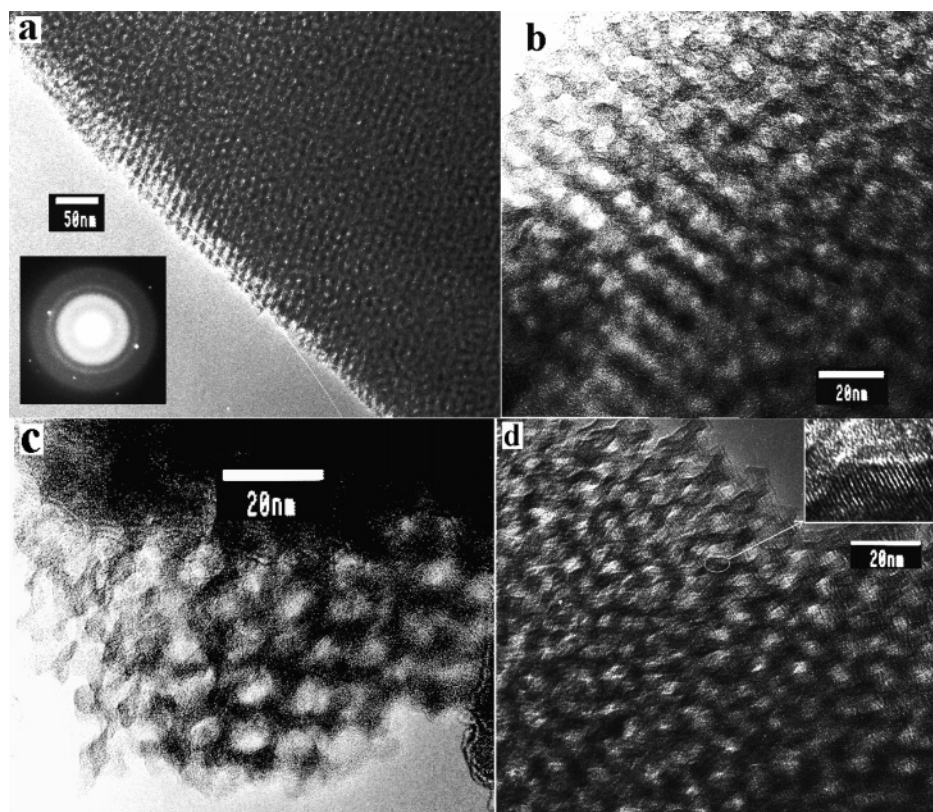


Figure 2. TEM images of the mesoporous TPO nanocomposite thin film. Two samples were examined: (a,d) for sample A; (b,c) for sample B. Inserts in (a) and (d) show the selected-area electron diffraction pattern and the lattice fringes.

films. TEM images in Figure 2 clearly show the periodical arrangement of mesopores. From the images in Figure 2b,c, the pore-to-pore spacing was determined to be ~ 10 nm, approximately 2 times as large as that derived from XRD. A combination of the TEM and XRD results reveals that ordered mesoporous TPO nanocomposite films contain a body-centered cubic (bcc) mesostructure, and the diffraction peak in Figure 1A can be indexed as (200).¹⁰ Note that there is no signal from ($n00$) planes with odd values of n for the bcc structure. The earlier work shows that, for ordered mesoporous powder samples with a bcc mesostructure, the (110) peak can be easily detected.¹¹ However, with our films, the (110) peak was not observed at the predicted position $2\theta \approx 1.26^\circ$, giving a sign that the film has a preferred orientation with the (100) plane of the bcc mesophase being parallel to the film surface. As a matter of fact, such an orientation has been discovered earlier with bcc-

mesostructured mesoporous SiO_2 and TiO_2 thin films prepared with the P123 template.¹⁰ From the point of view of molecular diffusion and adsorption, it is evident that a cubic-mesostructured mesoporous thin film with interconnected pores is more effective and advantageous than a two-dimensional hexagonal mesoporous film in which pore channels are arranged parallel to the substrate.³ Both the selected-area electron diffraction pattern and the lattice fringes shown in the inserts in Figure 2a,d reveal that the inorganic framework of the ordered mesoporous TPO nanocomposite film contains anatase- TiO_2 nanoparticles. In addition, the TEM images clearly indicate the presence of an amorphous component in the framework. The amorphous component should be titanium phosphate, which, according to our previous work,¹² plays vital roles of suppressing growth of TiO_2 nanoparticles and preventing collapse of the ordered mesostructure during calcination. Figure 3 depicts

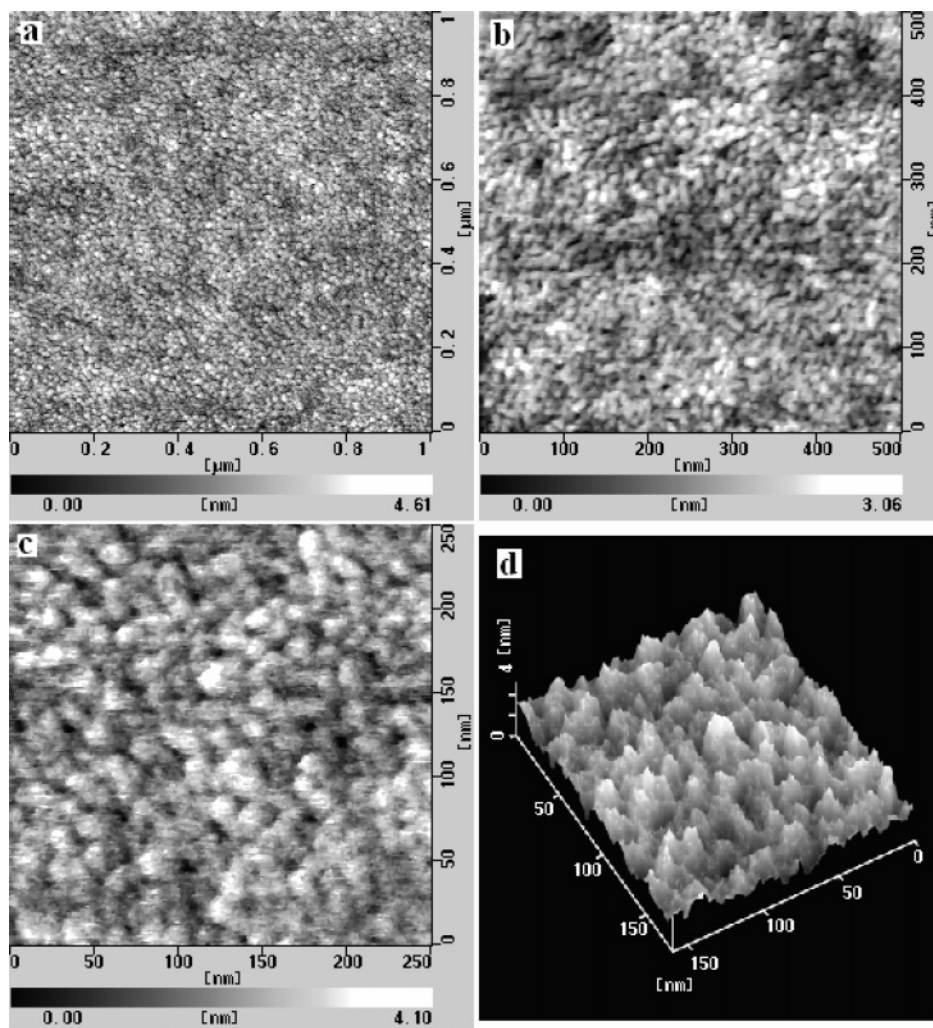


Figure 3. AFM images of the mesoporous TPO nanocomposite thin film. (a) $1\ \mu\text{m} \times 1\ \mu\text{m}$; (b) $500\ \text{nm} \times 500\ \text{nm}$; (c) $250\ \text{nm} \times 250\ \text{nm}$; (d) a 3D view of a selected region in (c).

tapping-mode AFM images of the mesoporous TPO nanocomposite thin film on the glass substrate. The film is smooth and crack-free, and the open pore mouths are discernible, but the ordered mesostructure is ambiguous on the film surface.

To demonstrate waveguiding, the glass substrate was mounted on a rotating stage, two glass prisms with $n = 1.81$ at 633 nm were attached to the mesoporous TPO nanocomposite thin film with a refractive-index-matching liquid (CH_2I_2 , $n = 1.73$), and a He–Ne laser beam was incident upon a prism. At a given incident angle, the laser light was launched into the thin film to propagate inside the film. Owing to surface scattering, a bright red streak was observed along the propagating path (Figure 4a). At the end of the thin film, that is 5 cm apart from the input prism coupler, the streak stopped and a bright spot appeared. Careful investigations indicate that the surface streak can be observed only with the mesoporous TPO nanocomposite film coated on the tin-rich side of the float glass substrates. The thin film on the opposite side of the substrate could not show a red streak at any angle of incidence. It suggests that the core of the waveguide is not only the ordered mesoporous TPO nanocomposite film but also includes the tin-diffused layer being intrinsic to float glass slides.^{3,4} By measuring the scattered light intensity (I_s) along the surface streak using a fiber connected to a photodetector, a linear dependence of $\log(I_s)$ on the propagating distance (L) was obtained (Figure 4b). From the relation: $\log(I_s) = -0.1\alpha L + C$, where α is the propagation loss and C is a constant, α was determined to be 2.88 dB/cm. Such a relatively

low loss, attributable to the bilayer-core structure, renders the waveguide useful for chemical sensing.

Chemical gas-sensing application of the waveguide was carried out with single-beam polarimetric interferometry that measures induced changes in the phase difference ($\Delta\phi$) between fundamental transverse electric (TE_0) and magnetic (TM_0) modes guided in the waveguide.^{3,4} As shown in Figure 5a, the experimental setup was built by covering the middle region of the ordered mesoporous TPO nanocomposite thin film with a 2-cm-long gas chamber and passing the incident and output light through a 45° polarizer and a 45° analyzer, respectively. After simultaneously flowing dry air (150 mL/min) and pure nitrogen (40 mL/min) through the gas chamber, the output light was monitored using a pinhole photodetector. The detected light intensity (I) is related to $\Delta\phi$ by eq 1, and $\Delta\phi$ is a function of the difference between two modal indexes, N_{TE} and N_{TM} , for the TE_0 and TM_0 modes.

$$I = I_0[1 + \cos(\Delta\phi)] \quad (1)$$

$$\Delta\phi = (2\pi L/\lambda)(N_{\text{TE}} - N_{\text{TM}}) \quad (2)$$

where L is length of the mesoporous film in the gas chamber ($L = 2\ \text{cm}$) and λ is wavelength ($\lambda = 633\ \text{nm}$). Owing to the different dependences of both N_{TE} and N_{TM} on refractive index of the ordered mesoporous TPO film, molecular adsorption-induced changes in the film index of refraction would cause

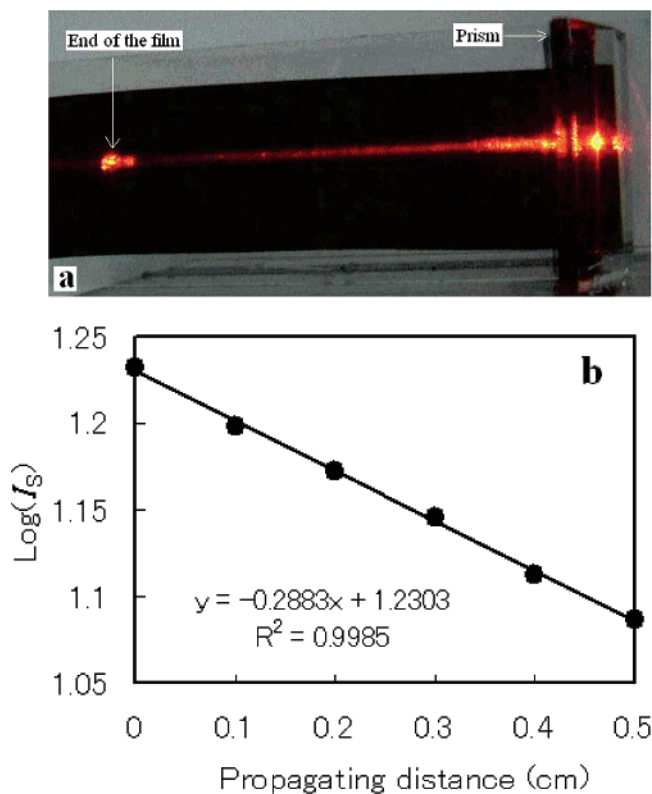


Figure 4. (a) Surface streak observed along the mode-propagating path. (b) Scattered light intensity versus the mode-propagating path length (filled circles, experimental data points; straight line, fitting curve with the equation $y = -0.2883x + 1.2303$. Goodness of fit is $R^2 = 0.9985$).

$\Delta\phi$ to vary. Once the signal stabilizes with time, pure N_2 is replaced with 10 ppm of NH_3 in N_2 , leading to exposure of the mesoporous TPO nanocomposite thin film to 2.1 ppm of NH_3 . Figure 5b shows the response of the waveguide. The NH_3 exposure causes the output light intensity to decrease with time within 6 min, evidencing adsorption of NH_3 molecules within the ordered mesoporous TPO nanocomposite film. Switching from NH_3 to N_2 leads to a slow increase of the light intensity, indicating that the adsorbed NH_3 molecules can be slowly removed from the mesoporous film. It is clear that the waveguide response to NH_3 is quasi-reversible and almost reproducible. For cubic-mesostructured mesoporous thin films with interconnected pores and open pore mouths on the film surface, the response time of the waveguide-based sensors is related with the film thickness: the thinner the film, the faster the response. With the polarimetric interferometry, the sensor response also depends on the initial phase difference (i.e., $\Delta\phi$ prior to the gas exposure). For the present setup with separate optical elements, the initial $\Delta\phi$ is not fixed. Therefore, the output light intensity sometimes increases upon exposure to the same concentration of NH_3 . For example, Figure 5c shows that the sensor response to NH_3 is opposite to that in Figure 5b. The sensor response to 2 ppm of C_6H_6 vapor in N_2 was also shown in Figure 5c. Extremely similar to our previous work,⁴ exposure of the mesoporous TPO film to C_6H_6 causes a pulse change rather than a fixed one in the light intensity. This indicates that the sensor is insensitive to C_6H_6 , perhaps due to the inability of nonpolar C_6H_6 molecules to stably adsorb to the pore wall of the mesoporous TPO film. The C_6H_6 insensitivity may suggest that the present sensor is immune to interference from nonpolar gases. However, when the sensor is used for ammonia detection, the cross-sensitivity to other polar gaseous molecules such as water vapor has to be taken into account. Our

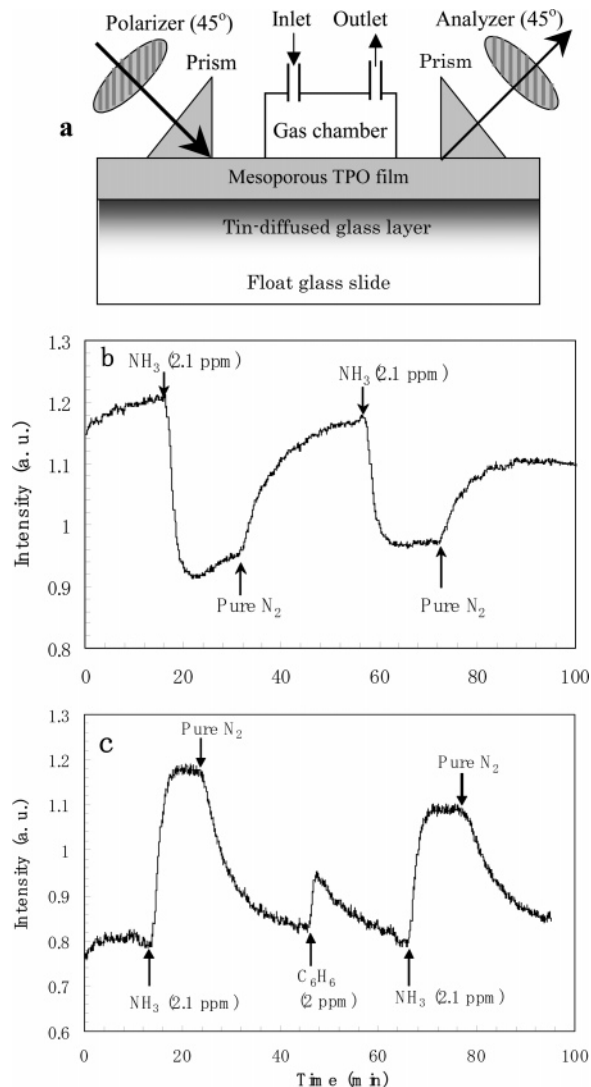


Figure 5. (a) Experimental setup for measuring gas-sensing properties of the planar optical waveguide based on polarimetric interferometry. (b,c) Responses of the waveguide to 2.1 ppm of NH_3 in dry air at room temperature. The different responses in (b) and (c) are ascribed to the different initial phase differences in both measurements.

measurements illustrated in Figure 5b,c give a primary demonstration that optical waveguides fabricated with ordered mesoporous thin films are an effective tool for chemical sensings at room temperature.

In conclusion, uniform, transparent and cubic-mesostructured mesoporous thin films of TPO nanocomposite were fabricated and successfully used for optical waveguiding and interferometric gas sensing at room temperature. The demonstrated applications point out a new and effective approach to ordered mesoporous thin-film waveguide-based optical chemical sensors.

Supporting Information Available: A further comparison between the sensor responses to NH_3 gas and C_6H_6 vapor. This material is available free of charge via the Internet at <http://pubs.acs.org>.

References and Notes

- (1) Fabricius, N.; Gauglitz, G.; Ingenhoff, J. *Sens. Actuators, B* **1992**, 7, 672.
- (2) Cross, G.; Reeves, A.; Brand, S.; Swann, M.; Peel, L.; Freeman, N.; Lu, J. *J. Phys. D: Appl. Phys.* **2004**, 37, 74.
- (3) Qi, Z.; Honma, I.; Zhou, H. *Appl. Phys. Lett.* **2006**, 88, 053503.

- (4) Qi, Z.; Honma, I.; Zhou, H. *Anal. Chem.* **2006**, 78, 1034.
- (5) Matsubara, K.; Kawata, S.; Minami, S. *Opt. Lett.* **1990**, 15, 75.
- (6) Horvath, R.; Pedersen, H. C.; Cuisinier, F. J. G. *Appl. Phys. Lett.* **2006**, 88, 111102.
- (7) Lau, K. H. A.; Tan, L.; Tamada, K.; Sander, M. S.; Knoll, W. *J. Phys. Chem. B* **2004**, 108, 10812.
- (8) Han, Y.; Stucky, G. D.; Bulter, A. *J. Am. Chem. Soc.* **1999**, 121, 9897.
- (9) Brinker, C. J.; Lu, Y.; Sellinger, A.; Fan, H. *Adv. Mater.* **1999**, 11, 579.
- (10) Alberius, P. C. A.; Frindell, K. L.; Hayward, R. C.; Kramer, E. J.; Stucky, G. D.; Chmelka, B. F. *Chem. Mater.* **1998**, 12, 3284.
- (11) Tian, B.; Liu, X.; Tu, B.; Yu, C.; Fan, J.; Wang, L.; Xie, S.; Stucky, G. D.; Zhao, D. *Nat. Mater.* **2003**, 2, 159.
- (12) Li, D.; Zhou, H.; Honma, I. *Nat. Mater.* **2004**, 3, 65.